NEW APPLICATIONS IN THE INVERSION OF ACOUSTIC FULL WAVEFORM LOGS – RELATING MODE EXCITATION TO LITHOLOGY

by

Frederick L. Paillet

U.S. Geological Survey
Denver, CO 80225

C.H. Cheng and J.A. Meredith

Earth Resources Laboratory
Department of Earth, Atmospheric, and Planetary Sciences
Massachusetts Institute of Technology
Cambridge, MA 02139

ABSTRACT

Existing techniques for the quantitative interpretation of waveform data have been based on one of two fundamental approaches: 1) simultaneous identification of compressional and shear wave velocities; and 2) least-squares minimization of the difference between experimental waveforms and synthetic seismograms. Techniques based on the first approach do not always work, and those based on the second seem too numerically cumbersome for routine application during data processing. An alternative approach is tested here, in which synthetic waveforms are used to predict relative mode excitation in the composite waveform. Synthetic waveforms are generated for a series of lithologies ranging from hard, crystalline rocks (V_p = 6.0 km/s and Poisson's ratio = 0.20) to soft, argillaceous sediments (V_p = 1.8 km/s and Poisson's ratio = 0.40). The series of waveforms illustrates a continuous change within this range of rock properties. Mode energy within a characteristic velocity window is computed for each of the modes in the set of synthetic waveforms. The results indicate that there is a consistent variation in mode excitation in lithology space that can be used to construct a unique relationship between relative mode excitation and lithology.

INTRODUCTION

Acoustic waveform logging has been a subject of intense research over the past decade, but progress in the computerized processing of waveform data has been relatively slow. Almost all of the existing computer programs for waveform logging rely upon either a combination of shear and compressional velocity picking (Geyer and Myung, 1970;

Willis and Toksöz, 1983) or qualitative interpretation of plotted waveforms (Cheng and Toksöz, 1981; Toksöz et al., 1985). Experience has demonstrated that shear wave velocities cannot always be effectively recognized by any given data processing scheme. Shear wave arrivals are not present in waveform data when shear wave velocity drops below the acoustic velocity of the borehole fluid. In the latter case, tube-wave velocities can sometimes be used to calculate shear wave velocity according to the equation given by White (1965), if the theory is extended to higher frequencies and the effects of velocity dispersion are included (Cheng and Toksöz, 1983; Stevens and Day, 1986). Even the tube-wave method for inferring the shear wave velocity of "slow" formations will not work if logging sources do not contain the low frequencies required to generate tube waves in some rocks. Because other wave modes may sometimes be misidentified as tube waves, the inference of shear wave velocity from calculated tube-wave speed will depend upon the correct identification of tube waves in the acoustic record. In permeable formations, this method fails because of the added effect of permeability on the phase velocity of the tube wave (Williams et al., 1984; Burns and Cheng, 1986).

The theory of wave propagation in homogeneous solids indicates that all elastic properties of a solid can be calculated if compressional and shear wave velocities are known, and if bulk density is given by some other measurement, such as the compensated density log. If shear wave velocities cannot always be reliably picked from the acoustic waveforms obtained in boreholes, then one alternative is to compare synthetic waveforms with the waveform log to determine the set of elastic constants that produces the best fit. Cheng and Toksöz (1981) and Toksöz et al. (1985) indicate that this is possible in theory, and that good fits can be obtained in typical petroleum reservoir rocks. However, the synthetic-waveform theory is complicated, and iterative computation of synthetic waveforms to match a specified data set would be far too cumbersome for routine application. An alternative approach might be to compare waveform logs with tabulated sets of synthetic data, but such a process still would be very time consuming. An additional complication would be added by the dependence of waveforms on source spectrum. Tabulated synthetic data could be convolved with different source models for each data set as part of the inversion process. In practice, the waveform-matching procedure is performed qualitatively according to the judgement of the log analyst comparing synthetic waveforms with waveform logs. The processes involved in such subjective matching are beyond the capacity of most modern computers, and must await the perfection of the artificial-intelligence algorithms of the future.

This study describes an alternative approach to either the shear-wave-velocity-picking or waveform-matching procedures described in the waveform-logging literature. The general objective is to identify a method for the interpretation of lithology and seismic velocities that is not dependent upon shear wave arrival detection, yet is not as computationally cumbersome as the point-by-point matching of actual with synthetic waveforms. The method is based on the hypothesis that the relative energy of specific acoustic modes of vibration can be predicated by theory. Examples are described in terms of excitation curves by Paillet and White (1982). Cheng and Toksöz (1981) described the effect of different relative excitations on the character of composite wave-

form. One specific result of their calculation was the sensitivity of wave energy arriving after the first compressional wave arrival to the Poisson's ratio of the rock. Calculation of energy ratios in different parts of recorded waveforms seems to offer a reasonable compromise between the requirements of computational efficiency and the possibility of pointwise matching of waveforms as demonstrated by Cheng and Toksöz (1981).

A simple example of the partitioning of waveform logs into individual wave modes is shown in Figure 1 (Paillet, 1980, 1983). The inverse problem of identifying the seismic velocities for a given waveform was relatively simple in the example because shear wave velocities would be picked from the waveforms, and theory indicated that all waveforms should be dominated by a large-amplitude tube wave at the applied source-frequency band. Amplitude logs were generated by gating the energy in a specific velocity window. The amplitude logs described by Paillet (1980) used a half-cosine filter, but specific filter choice apparently was not critical. In practice, some general knowledge of rock properties is needed to determine velocity windows for wave modes. However, reliable values of compressional velocity will be available from acoustic logs along with bulk density from nuclear logs, so estimates of mode velocities can be made as the first step in a convergent iteration.

WAVE MODES IN BOREHOLES

Detailed discussions of wave modes in boreholes have been presented in numerous reports (for example, Biot, 1952; Peterson, 1974; Paillet and White, 1982). Perhaps the most important point is that waveform logs record waves that have propagated along the borehole. Recorded waveforms are composed of various guided modes that represent acoustic energy trapped or partially trapped in the borehole. At the same time, geometric-ray theory cannot be applied to borehole microseismograms because the ratio of acoustic wavelength to borehole diameter usually is greater than one, and finite wavelengths need to be used to calculate borehole responses. None of the energy arriving at the logging-tool receivers can be regarded as propagating as simple body waves in an elastic solid. A detailed review of the relationship between compressional and shear wave arrivals in acoustic waveforms and guided modes is given by Kurkjian (1985) and Paillet and Cheng (1986). The most important conclusion from this theory is that virtually all acoustic energy arriving at the logging-tool receivers can be related to the amplitude of one or more of the guided wave modes.

The composite waveform recorded by the logging system is the sum of contributions from two groups of normal modes (compressional and shear) and the tube wave. The contributions from the normal modes can be further divided into contributions greater or less than cutoff frequencies. Such divisions are natural because the mode cutoffs correspond to guided propagation either above or below the critical angle of refraction. At frequencies greater than cutoff (corresponding to refraction angles greater than critical) all wave energy is refracted along the borehole, and guided waves are not attenuated. At

frequencies less than cutoff, wave energy leaks by outward radiation, so these modes are attenuated. Numerical calculations indicate that the amplitude of arrivals denoted as compressional and shear waves are determined by the amplitude of modes below cutoff (Kurkjian, 1985; Paillet and Cheng, 1986). The separation of modes into branches at frequencies greater or less than cutoff is also a natural division because energy arguments and direct calculations indicate that mode amplitudes go through zero at cutoff frequencies. A summary of modes and their properties is given in Table 1.

One of the greatest problems in associating the amplitude of wave modes with the shape of waveforms is the tendency of researchers to produce excitation curves suitable for input into mathematical models rather than for data interpretation. Excitation curves typically are plotted as a function of frequency for a specific set of borehole conditions and seismic velocities. These amplitude spectra can then be used to construct synthetic microseismograms using Fourier-transform methods as described by White and Zechman (1968), Rosenbaum (1974), and Cheng and Toksöz (1981). An example is given in Figure 2, where shear-normal-mode dispersion and excitation curves are given for the shear-normal-mode frequency greater than cutoff. The data in the figure indicates that mode energy becomes divided among progressively more shear normal modes as frequency increases, whereas the tube wave is a relatively small part of the total excitation at frequencies greater than 10 kHz. The group velocities derived from the dispersion curves for these modes further indicate that there will be a concentration of energy arriving at velocities equal to or less than the acoustic velocity of the borehole fluid, and having a abrupt end corresponding to the minimum group velocity (the so-called Airy phase). All of this information is very relevant to the Fourier synthesis of waveforms, but the plotting of dispersion curves in frequency and wavenumber space makes these curves difficult to apply to waveforms recorded in time at a fixed point uphole from an acoustic-energy source.

Some insight into the effects of lithology on acoustic-waveform character can be obtained by studying dispersion curves such as those in Figure 2 for different rock types. An example of mode dispersion in shale is shown in Figure 3, where the dispersion and excitation curves for a compressional mode at a frequency greater than cutoff is given at various Poisson's ratios. The Poisson's ratio has been varied by keeping a constant compressional wave velocity, and decreasing the shear wave velocity. A fourth curve has been plotted in Figure 3 because the mode-damping factor needs to be taken into account. That is, the frequency range greater than cutoff allows the mode to propagate without radiation of compressional wave energy, but radiation of shear wave energy into the surrounding rock still occurs. Hence this mode has been designated the leaky compressional normal mode or PL-mode in the literature (Phinney, 1961). The figure indicates that PL-mode (part of the compressional-mode trajectory at frequencies greater than cutoff) amplitude increases markedly, whereas PL-mode damping decreases as the Poisson's ratio increases for rocks with these seismic velocities. A similar dependence of PL-mode amplitude on Poisson's ratio was noted by Cheng and Toksöz (1981) for rocks with greater compressional velocities.

Calculations described by Paillet and Cheng (1986) indicate that energy contribution to compressional and shear waves occurs for a restricted frequency range just less than mode cutoff. An experimental verification of this result is illustrated in Figure 4. These waveforms were obtained using an acoustic source restricted to frequencies far less than mode cutoff. The recorded waveforms were composed almost entirely of tube-wave energy. There were only slight indications of compressional and shear wave arrivals characterized by the higher cutoff frequencies when records were made at the maximum possible gain setting. Most commercially available logging sources have frequencies in which the source band is dominated by only one set of mode cutoffs at typical logging conditions. In that case, compressional- and shear-wave amplitude can be related to the excitation of that single set of modes at frequencies just less than mode cutoff.

SCALING BOREHOLE WAVEFORMS

Acoustic waveform logs contain a great deal of information about rock properties, but waveform logs (as any given geophysical-log measurement) do not uniquely define lithology. According to theory, waveforms for a specific rock type are determined using a few constants: compressional and shear wave velocities of the rock, compressional wave velocity of the borehole fluid, rock and fluid densities, and borehole diameter. In some instances, the boundary conditions at the center of the borehole are replaced by boundary conditions at the rigid surface of a logging tool. The character of waveforms is only slightly dependent on the ratio of fluid density to rock density (Paillet and White, 1982), and most waveform variation with tool and borehole radii is accounted for by the single parameter of annulus width (Cheng and Toksöz, 1981).

The greatest variation in waveforms with lithology may, thus, be accounted for by only four parameters: the three velocities (compressional, shear, and fluid) and annulus width. If annulus width and the acoustic velocity of the borehole fluid are known, then waveform inversion is reduced to inferring Poisson's ratio (and hence shear wave velocity) from waveform character. This virtually is the method proposed by Cheng and Toksöz (1981) based on the observed dependence of synthetic waveforms on Poisson's ratio.

Superimposed on the effects of seismic velocities and annulus width are the effects of acoustic-source character, source-to-receiver separation, and intrinsic attenuation. Acoustic source character can apparently have a major effect on the appearance of waveforms, but it is unclear how details of the source signal affect the ability to match synthetic waveforms with waveform logs. Many existing logging tools use relatively narrow-band sources because velocity picks are made by calculating the time lag between consistent phases at two points up hole from the source. A minimum source-to-receiver separation usually is required to ensure that waveforms attain the far-field form predicted from theory. A minimum separation also is required to ensure that wave modes are sufficiently separated in the record to allow interpretation. Intrinsic

attenuation usually decreases over-all waveform amplitude, but does have some effect on waveform appearance, and on the qualitative identification of lithologies.

An entirely separate issue in the interpretation of waveforms is the question of depth of penetration around the borehole. Some authors (Baker, 1984) have cited geometric-ray theory to show that depth of penetration is dependent on source-to-receiver separation. Such calculations are only relevant when there are radial seismic-velocity changes due to invasion or shale hydration. In these instances, the geometric-ray theory yields results that are approximately correct. However, nothing more can be gained once separation has increased to the point where the first arrivals penetrate beyond the invaded zone. This is not true if intrinsic attenuation is important, because attenuation systematically removes the shorter wavelengths from the waveform log. As a result, separation will continue to provide deeper penetration indefinitely because seismic wavelengths increase continuously with source-receiver separation. There also will be relative amplitude changes associated with increasing separations because each mode is subjected to losses by various degrees of radiation and dispersion greater than intrinsic attenuation.

Seismic velocities of the rocks encountered in well logging range from a maximum of more than 6.0 km/s compressional and 4.0 km/s shear wave velocities to a minimum in which both velocities are less than the acoustic velocity in the borehole fluid. If the acoustic velocity in the fluid is used as a scale, then this range is:

$$1.0 \leq V_p/V_f \leq 4.0 \ \ and \ \ 0.0 < V_s/V_f \leq 3.0 \tag{1}$$

However, rock seismic velocities almost never vary throughout this full range. For example, Castagna et al. (1985) have investigated the effects of porosity and shale content on seismic velocities for sandstone. They reported that all velocities tended to plot upon a mudrock line as indicated in Figure 5. Crystalline and metamorphic rocks tend to have faster velocities and smaller Poisson's ratios, as indicated by the values for granite and basalt in Figure 5. Sedimentary-rock types incorporating carbonate rocks into the mineral matrix produce points that plot somewhat off the main mudrock line, but still follow the same trend. We have expanded the trend discussed by Castagna et al. (1985) to include carbonate, igneous, and metamorphic rocks. The data plot within a band containing the mudrock line. We hereafter designate this trend containing the mudrock line of Castagna et al. (1985) as the lithology band in seismic-velocity space.

In summary, the parameters that govern the character of synthetic waveforms in boreholes indicate that the primary effects of lithology on waveforms can be represented by variation along the lithology band indicated in Figure 5. That is, a series of synthetic waveforms can be developed to interpret lithology from waveform logs by a single spectrum of master waveforms. This synthetic data set would span the parameter range defined by the simultaneous limits

$$1.0 \leq V_p/V_f \leq 4.0 \ \textit{and} \ 0.45 \geq \nu \geq 0.2 \qquad (2)$$

Some additional variation will occur because of attenuation, source-to-receiver separation, and source-frequency effects, but the primary effect of lithology on waveform appearance should be accounted for by means of this one spectrum of waveform types.

MODE AMPLITUDE AND LITHOLOGY

The primary objective of this study is the development of relative excitation curves that can be directly applied to waveform-log interpretation. Diagrams plotting mode excitation and dispersion as a function of frequency such as those shown in Figure 1b appear difficult to apply to the interpretation of lithology. Some insight into relative mode excitation can be obtained by comparing several such curves for different seismic velocities, as in Figure 3; however, the most direct comparison of waveform logs can be obtained by plotting excitation curves and sample waveforms for various velocity combinations along the lithology trend illustrated in Figure 5. Additional curves and waveforms can then be calculated to indicate how the effects of intrinsic attenuation and source-to-receiver separation modify this single major trend.

The first obstacle to overcome when attempting to transform mode excitation from frequency space to lithology space is the source frequency band. The borehole itself provides the information needed in resolving this issue. Calculations by Kurkjian (1985) and Paillet and Cheng (1986) indicate that all contributions to shear and compressional waves occur for the limited frequency range just less than mode cutoff. Acoustic logging equipment has evolved to include source spectra centered on the cutoff frequencies for the first compressional and shear modes. For borehole diameters ranging from 15 to 30 cm, these frequencies correspond to the frequency range of 10 to 20 kHz. Such frequencies apparently have been used because geophysicists found that they produced the best results during conventional acoustic logging, but the natural response of the borehole tends to produce frequency outputs centered on the band in the vicinity of the first pair of mode cutoffs. This results from the combined effects of mode excitation and the increased attenuation of higher-frequency modes excited by the acoustic source. However, mode excitation under a wide variety of conditions can be effectively modeled by using an assumed energy source with a bandwidth centered on the cutoff frequencies for the first pair of compressional and shear modes. The energy source and associated amplitude spectrum used to construct synthetic waveforms in this study are shown in Figure 6.

After assuming the energy source in Figure 6, synthetic waveforms were produced for a series of plots along the trend indicated by equation 2. Seismic velocities and borehole diameters modeled for these cases are summarized in Table 2. Note that the assumed-source centerband frequency was set to include the first compressional-mode

cutoff, and that the band was made wide enough to include the first shear cutoff for all but the lowest velocity cases, where shear excitation becomes relatively unimportant. Source-to-receiver spacing was selected to represent a few wavelengths at the source centerband frequency. Sample waveforms at eight points along the lithology trend in equation 2 are shown in Figure 7a–h. Waveform amplitude has been normalized for the illustration of waveform character in Figure 7. Actual amplitudes increase continuously from Figure 7a to 7h.

Mode excitation curves for a series of synthetic waveforms such as those in Figures 7a–h were calculated by gating arriving wave energy in appropriate time windows. This virtually is the same procedure described by Paillet (1980, 1983) for the calculation of tube-wave-amplitude logs. Wave-mode amplitudes represent the mean wave energy in the specified time window. This corresponds numerically to the squared amplitude at each digitized point convolved with a half-cosine filter, and divided by the number of points in the time window. Time windows used for the amplitude calculations are summarized in Table 3.

Mode amplitudes constructed from synthetic waveforms specified by the seismic velocities in Table 2 using the time windows in Table 3 are plotted in Figure 8. All amplitudes have been scaled by plotting the ratio of the windowed amplitude to the amplitude in the compressional window. The data in the figure indicate a general trend of decreasing mode amplitudes as Poisson's ratio increases. This trend is related to the effectiveness of the borehole as a seismic-wave guide. The borehole is a more efficient transmitter of guided waves when there is a greater contrast between the seismic velocities of the rock and the acoustic velocity of the borehole fluid. The leaky compressional or PL-mode trend seems to contradict the trend of increasing amplitude with increasing Poisson's ratio as reported by Cheng and Toksöz (1981). This result is partly because of the plotting method, and partly because of the effect of the compressional leaky mode in exciting the compressional head wave (Paillet and Cheng, 1986). The slope of the excitation curves for the PL-mode and for the shear head wave in Figure 8 indicates that the ratio of PL to shear amplitude does increase with increasing Poisson's ratio. The compressional-mode and the PL mode amplitude increase simultaneously with increasing Poisson's ratio, so the ratio of the two modes does not indicate the increased efficiency of excitation of both as described by Cheng and Toksöz (1981).

The shear-head-wave amplitude indicated a marked decrease with increasing Poisson's ratio in Figure 8, but the trend is complicated by a reversal at intermediate values. Inspection of the complete waveform for this case indicates a single coherent packet of wave energy in the vicinity of shear arrival time, and there is no indication of a shear normal mode. This waveform shape indicates that the local increase in shear-wave amplitude in Figure 8 is related to the coincidence of shear normal mode cutoff frequencies with the spectral peak of the synthetic source. A similar effect would occur for the compressional mode at even larger values of Poisson's ratio, except such an effect is masked by the normalization procedure used in this study. The near resonance condition that exists in this situation would be greatly decreased by the introduction of

intrinsic attenuation.

The shear-normal-mode and tube-wave mode amplitude in Figure 8 seems to decrease continuously with increasing Poisson's ratio. The interpretation is somewhat complicated by the superposition of the Airy phase of the shear normal mode and tube wave in the same velocity window. This can be treated in a practical fashion by recognizing that the Airy phase will dominate at all larger values of V_p, whereas the tube-wave velocity in slow formations allows the tube wave to lag behind the amplitude window. Therefore, the Airy-phase and shear-normal-mode windows produce amplitude trends that are nearly parallel for values of $V_p \geq 4.5$ km/s. Theory indicates that identifiable tube waves are present because of either unusual logging conditions where source frequencies are substantially less than cutoff for all modes (Figure 4) or because of slow formations where tube waves lag far behind other arrivals. In the latter case, the prominence of the late tube-wave arrival is due to excitation as a function of frequency in slow formations. Tube-wave excitations in fast and slow formations are compared in Figure 9. The excitation function for slow formation tube waves decreases rapidly with frequencies more than a few kilohertz. Slow-formation tube waves, therefore, need to be excited by the low-frequency sideband of the source, and propagate with the slow velocities characteristic of excitation at those frequencies.

The waveforms in Figure 7 are plotted on a uniform amplitude scale in approximately the format used in many full waveform data displays in Figure 10a. The waveforms indicate a progressive decrease in the energy of the shear normal mode Airy phase as shear-wave arrival time decreases towards fluid arrival, and cutoff frequency for the lowermost shear normal mode increases towards the source centerband frequency (about 12 kHz). The waveform for $V_p = 3.0$ km/s (top of right column in Figure 7) indicates the transition where shear mode cutoff coincides with source frequency, and most of the Airy phase frequencies (corresponding to the minimum in the group velocity curve) are greater than source excitation. At the same time, tube-wave excitation shifts towards lower frequencies (Figure 9) lagging behind the rest of the waveform. The prominence of this tube wave, thus, is caused by a combination of slower velocity and removal of the Airy phase.

At even larger values of Poisson's ratio, shear-wave arrival extends beyond fluid arrival, so that shear-normal-mode cutoff frequencies have effectively increased to infinity (i.e., there can be no total internal reflection when V_s is less than V_f). At the same time, the source frequency becomes tuned to the compressional mode, and tube-wave amplitude corresponds to the amplitude peak for slow formations in Figure 9. For the slowest formations, V_p is only slightly greater than V_f, and the waveform is completely dominated by the dispersive arrival of the fundamental compressional mode. The tube-wave amplitude has decreased, and the tube wave arrives after the time interval shown in the figure.

The waveforms illustrated in Figures 7a–h correspond to models generated without intrinsic attenuation. The intrinsic attenuation of real rocks varies, and may have some

effect on waveform character. As in the case of compressional and shear wave velocities, values for Q_p and Q_s vary along a general trend of decreasing Q as Poisson's ratio increases and V_p decreases (Toksöz et al., 1979; Johnston et al., 1979). To investigate the possible effects of attenuation on the waveform interpretation of lithology, the calculations were repeated with attenuation increasing as compressional velocity decreases such that $Q_p = 2Q_s$, with $Q_f = 100$. Values for Q_p were selected to correspond to those given by Toksöz et al. (1979) and Johnston et al. (1979) for sedimentary rocks (Table 2). Mode-excitation curves for synthetic waveforms with attenuation are compared to those without attenuation in Figure 11. The effect of attenuation is to decrease amplitudes for shear, shear normal mode, and Airy phase modes, while smoothing out the mid-range resonance peak in shear excitation.

A somewhat surprising result is the increase in shear normal mode excitation with attenuation. It appears that some of the wave energy that had been arriving in the Airy-phase window now arrives in the shear-normal-mode window. Much of the actual wave energy is conducted by the borehole fluid. We suspect that attenuation affects the propagation for the shear normal modes in such a way as to distort group velocity curves, and shift part of the mode energy forward in time.

Increasing source-to-receiver separation may have a similar effect on relative mode separation. The separation values used to compute the waveforms in Figures 7a–h and the excitation curves in Figures 8 and 11 were selected to correspond with the separations used in conventional acoustic-logging probes. Ultralong source-to-receiver separations recently have been recommended for waveform logging (Koerperich, 1979). The effect of such long separations was investigated by comparing the excitation curves calculated for increasing separations with those shown in Figure 8. These ultralong separations had a relatively minor effect on the relative excitation of wave modes. However, the synthetic waveforms were computed for a source band carefully selected to excite only the first pair of normal modes, and for formations that had uniform properties. Paillet and Cheng (1986) reported that the effectiveness of ultralong separations may be related to higher-frequency modes that are attenuated more than the first pair of modes in propagation over a finite spacing. Such higher-frequency modes have been removed from the synthetic data by restriction of source frequencies, and this attenuation effect is not apparent in Figure 12.

CONCLUSION

Almost all previous attempts to interpret acoustic waveform logs have been based on either the picking of shear-wave velocities, or on the careful matching of synthetic waveforms with digitized waveforms. At the same time, mode-excitation curves and waveform spectra usually have been plotted in frequency-wavenumber space in the Fourier synthesis of waveform models. Although such plots are important in understanding the theory of waveform propagation, they are very difficult to relate to specific rock

properties. Numerical interpretation of lithology based on waveform logs apparently will require a method that is more consistently reliable than shear-wave velocity picking, and yet is less cumbersome than point-by-point matching of model waveforms with data for specific source properties and borehole conditions.

Careful study of the seismic properties of rocks indicates that velocities and attenuation values plot along a general trend from fast-velocity crystalline rocks that have little attenuation and small Poisson's ratios to slow-velocity rocks with substantial attenuation and large Poisson's ratios. Unfortunately the trend representing increasing porosity in clean formations almost exactly parallels the trend representing increasing shale or clay content in shaley sands and carbonate rocks. Both trends plot along the mudrock line described by Castagna et al. (1985), and are within the broader lithology band described in this study.

An investigation of the properties of synthetic waveforms in homogeneous formations indicates that waveform amplitudes are determined by the relative excitation of shear and compressional normal modes, and the tube wave. The natural frequency response of the borehole superimposed on the tendency for propagation within a finite distance to attenuate higher frequencies indicates that mode excitation can be predicted by modeling the amplitudes generated by sources exciting the first compressional and shear modes.

The mode-excitation curves computed for the lithology band for the selected source frequencies indicate that there is a consistent trend in relative mode excitation with lithology. Attenuation has some effect on the character of these curves, but the known trend of increasing attenuation with decreasing seismic velocities probably can be used to account for this effect. Source-to-receiver separation seems to have only a minor effect on relative mode excitation in synthetic waveforms. Part of this result may be attributed to the removal of higher mode excitation by means of limiting the source frequency band in the synthetic waveforms, whereas real waveforms contain some sideband excitation of these higher frequency modes. Resonance conditions related to the coupling of source spectra to borehole response produce peaks in the amplitudes predicted by synthetic-waveform theory, but these peaks are decreased where intrinsic attenuation is introduced. These preliminary results otherwise indicate that relative mode excitation may be used as a relatively simple means to relate waveform logs to lithology.

ACKNOWLEDGEMENTS

This work was supported in part by the Full Waveform Acoustic Logging Consortium at M.I.T. J.A. Meredith is supported by a Chevron Fellowship.

REFERENCES

Baker, L.J., 1984, The effect of the invaded zone on full wave train acoustic logs; Geophysics, 49, 796-809.

Biot, M.A., 1952, Propagation of elastic waves in a cylindrical bore containing a fluid; J. Appl. Phys., 23, 997-1009.

Burns, D.R., and Cheng, C.H., 1986, Determination of in situ permeability from tube wave velocity and attenuation; Trans 27th SPWLA Ann. Logging Symp., in press.

Castagna, J.P., Batzle, M.L., and Eastwood, R.L., 1985, Relationships between compressional-wave and shear-wave velocities in clastic silicate rocks Geophysics, 50, 571-581.

Cheng, C.H., and Toksöz, M.N., 1981, Elastic wave propagation in a fluid-filled borehole and synthetic acoustic logs, Geophysics, 46, 1042-1053.

Cheng, C.H., and Toksöz, M.N., 1983, Determination of shear wave velocities in "slow" formations; Trans. 24th SPWLA Ann. Logging Symp., Paper V.

Cheng, C.H., Toksöz, M.N., and Willis, M.E., 1982, Determination of *in situ* attenuation from full waveform acoustic logs, J. Geophys. Res., 87, 5477-5484.

Geyer, R.L., and Myung, J.I., 1970, The 3-D velocity log – a tool for *in situ* determination of the elastic moduli of rocks, in Chapter 4, Dynamic Rock Mechanics; Proc. 12th Symp. on Rock Mechanics, 71-107.

Johnston, D.H., Toksöz, M.N., and Timur, A., 1979, Attenuation of seismic waves in dry and saturated rocks: II Mechanisms, Geophysics, 44, 691-711.

Koerperich, A.E., 1979, Shear wave velocities determined from long and short spaced borehole acoustic devices; Soc. Petro. Engr., Paper SPPE 8237.

Kurkjian, A.L., 1985, Numerical computation of individual far-field arrivals excited by an acoustic source in a borehole; Geophysics, 50, 852-866.

Nur, A, and Simmons, G., 1969, The effect of saturation on velocity in low porosity rocks; Earth and Plan. Sci. L., 7, 183-193.

Paillet, F.L., 1980, Acoustic propagation in the vicinity of fractures which intersect a fluid-filled borehole; Trans. 21st SPWLA Ann. Logging Symp., Paper DD.

Paillet, F.L., 1983, Acoustic characterization of fracture permeability at Chalk River,

Ontario; Can. Geotech. J., 20, 468-476.

Paillet, F.L., and Cheng, C.H., 1986, A numerical investigation of head waves and leaky modes in fluid-filled boreholes, Geophysics, in press.

Paillet, F.L., and White, J.E., 1982, Acoustic modes of propagation in the borehole and their relationship to rock properties; Geophysics, 47, 1215-1228.

Peterson, E.W., 1974, Acoustic wave propagation along a fluid-filled cylinder; J. Appl. Phys., 45, 3340-3350.

Phinney, R.A., 1961, Leaking modes in the crustal waveguide, Part 1: the ocean PL wave; J. Geophys. Res., 65, 1445-1469.

Rosenbaum, J.H., 1974, Synthetic microseismograms: logging in porous formations; Geophysics, 39, 14-32.

Toksöz, M.N., Cheng, C.H., and Timur, A., 1976, Velocities of seismic waves in porous rocks; Geophysics, 41, 621-645.

Toksöz, M.N., Johnston, D.H., and Timur, A., 1979, Attenuation of seismic waves in dry and saturated rocks : I. Laboratory measurements; Geophysics, 44, 681-690.

Toksöz, M.N., Wilkens, R.H., and Cheng, C.H., 1985, Shear wave velocity and attenuation in ocean bottom sediments from acoustic log waveforms; Geophys. Res. Lett., 12, 37-40.

White, J.E., 1965, Seismic Waves: Radiation, Transmission and Attenuation; McGraw-Hill Book Co.

White, J.E., and Zechman, R.E., 1968, Computed response of an acoustic logging tool; Geophysics, 33, 302-310.

Williams, D.M., Zemanek, J., Angona, F.A., Dennis, C.L., and Caldwell, R.L., 1984, The long space acoustic logging tool; Trans. SPWLA 25th Ann. Log. Symp., Paper T.

Willis, M.E., and Toksöz, M.N., 1983, Automatic P and S velocity determination from full-waveform digital acoustic logs; Geophysics, 48, 1631-1644.

Table 1 -- Wave modes in fluid-filled boreholes during typical logging conditions

PREFERRED NAME	ALTERNATE NAME	VELOCITY RANGE	COMMENTS
Compressional head wave	P wave	Narrow range near Vp	Spectral peak for frequency range just less than cutoff frequency
Leaky compressional normal mode	PL wave	Dispersed within range Vp to Vf	Amplitude depends on Poisson's ratio
Shear head wave	S wave	Narrow range near Vs	Spectral peak for frequency range just less than cutoff frequency
Shear normal mode	pseudo-Rayleigh wave	Dispersed within range Vs to Vf	
Airy phase of shear normal mode	Airy phase; "fluid wave"	Concentrated just after Vf	Associated with group velocity minimum
Tube wave	Stoneley wave	Ranges from 0.5 to 0.99 Vf	Velocity and amplitude sensitive to permeability

Table 2 -- Parameters used to calculate synthetic waveforms for rock properties characterized by variation along the lithology band in figure 5 (borehole diameter is 20 cm, borehole fluid density is 1.1 gm/cm3, and borehole fluid velocity is 1.5 km/s for all cases).

DENSITY (g/cm3)	POISSON'S RATIO	COMPRESSIONAL VELOCITY (km/s)	SHEAR VELOCITY (km/s)	Qp	Qs
2.60	0.20	6.0	3.70	100	50
2.55	0.21	5.5	3.33	80	40
2.50	0.22	5.0	3.00	70	35
2.45	0.23	4.5	2.67	60	30
2.40	0.25	4.0	2.31	50	25
2.35	0.27	3.5	1.96	45	22.5
2.30	0.30	3.0	1.60	40	20
2.20	0.33	2.5	1.24	35	17.5
2.10	0.37	2.0	0.91	30	15
2.00	0.40	1.8	0.74	*	*

* Attenuated waveforms not run for these cases.

Table 3 -- Time windows for gating amplitudes of wave modes.

Tc, Direct travel time at Vc (with fluid delay)

Ts, Direct travel time at Vs (with fluid delay)

Tf, Direct travel time at Vf

DTc, (Tf-Tc)

DTs, (Ts-Tc)

DTf, (Tf-Ts)

MODE	BEGIN WINDOW	END WINDOW	CENTERPOINT
Compressional	Tc - DTs/2	Tc + DTs/2	Tc
Leaky P	Tc	Ts	Tc + DTs/2
Shear	Ts - DTs/2	Ts + DTs/2	Ts
Shear Norm Mode	Ts	Tf	Ts + DTf/2
Airy/Tube	Tf	Tf + DTc	Tf + DTc/2

NOTE: Because gain of recorded waveforms is arbitrary, normalize energy levels with espect to compressional mode.

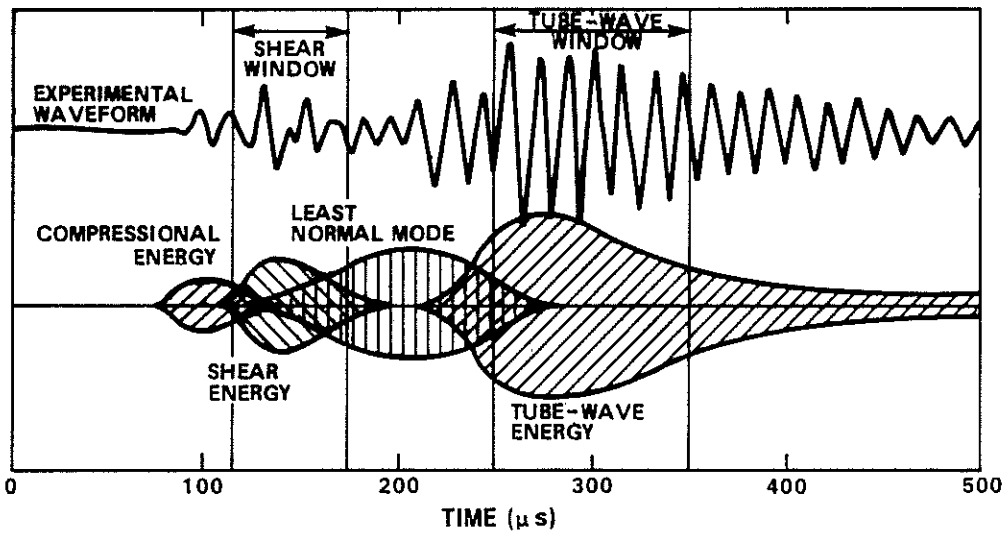

Figure 1: Example of partitioning of wave modes in acoustic waveforms for small borehole diameter in granite: a) waveform obtained with 34 kHz source; and b) predicted mode excitation.

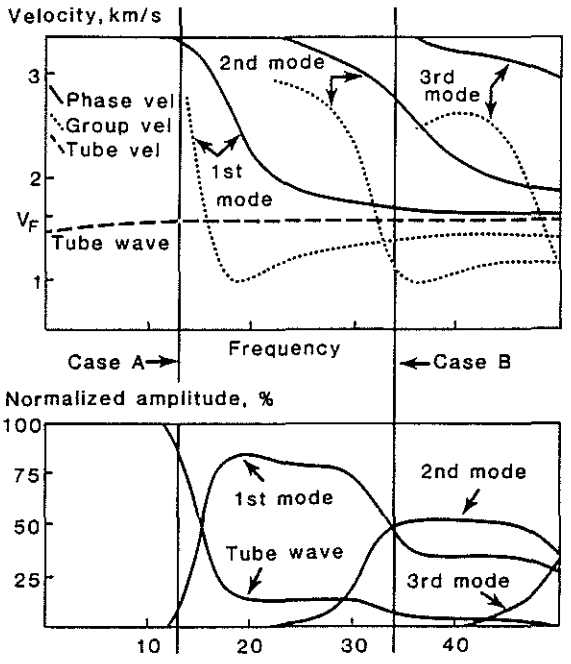

NORMAL BOREHOLE MODES-BASED ON A DIAMETER OF 200 cm

Figure 2: Shear-normal-mode dispersion and excitation curves for 20 cm diameter borehole in sandstone: a) phase and grape velocities; and b) relative mode excitation.

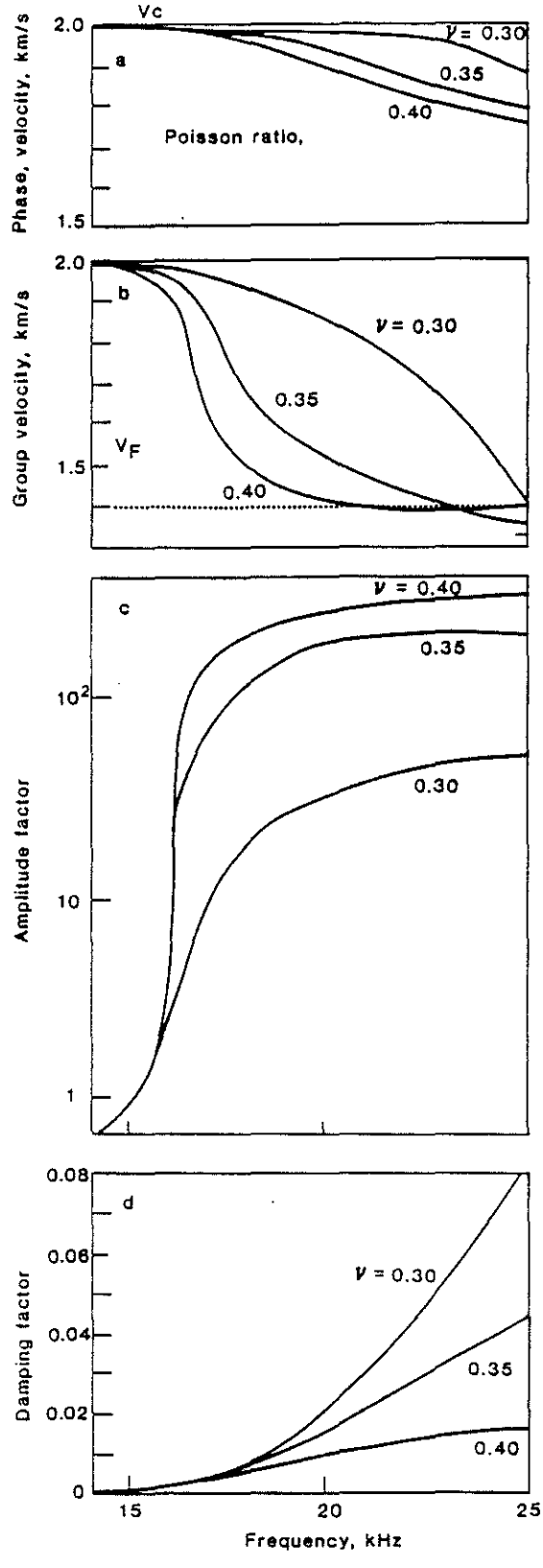

Figure 3: Effect of increasing Poisson's ratio for first compressional normal mode in a slow formation: a) phase velocities; b) group velocities; c) mode amplitudes; and d) mode damping factors for Poisson's ratios ranging from 0.3 to 0.4.

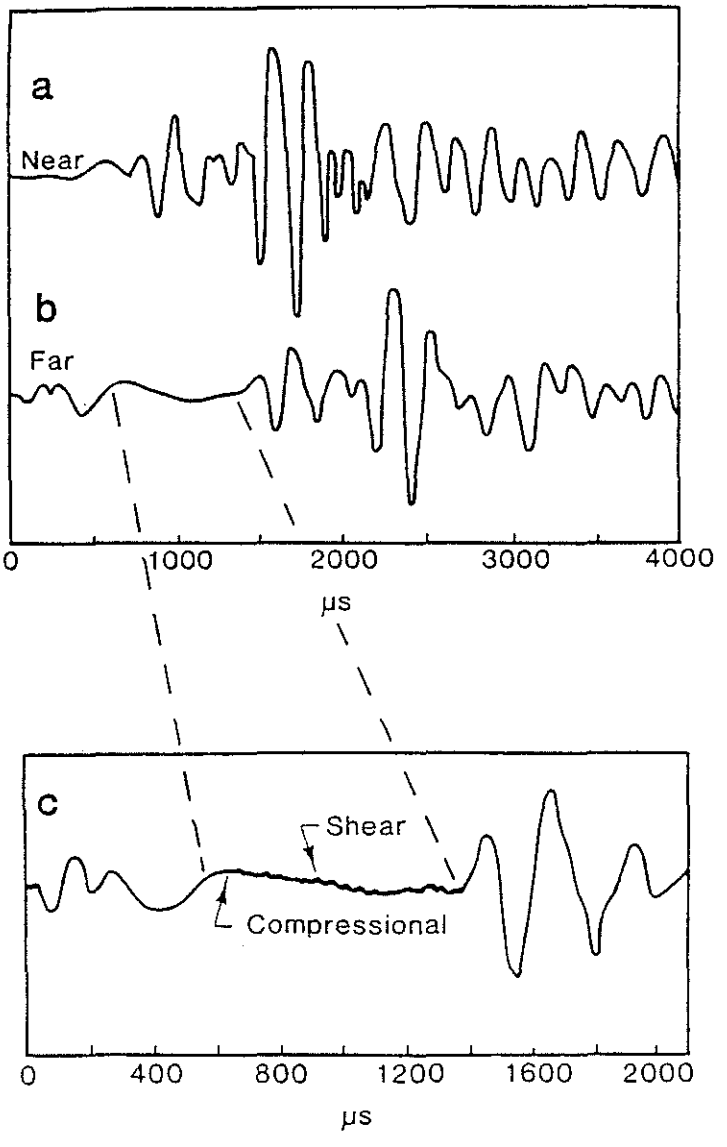

Figure 4: Waveforms obtained in granite using an experimental 5 kHz source illustrating poor excitation of compressional and shear waves with source energy at frequencies less than normal mode cutoff.

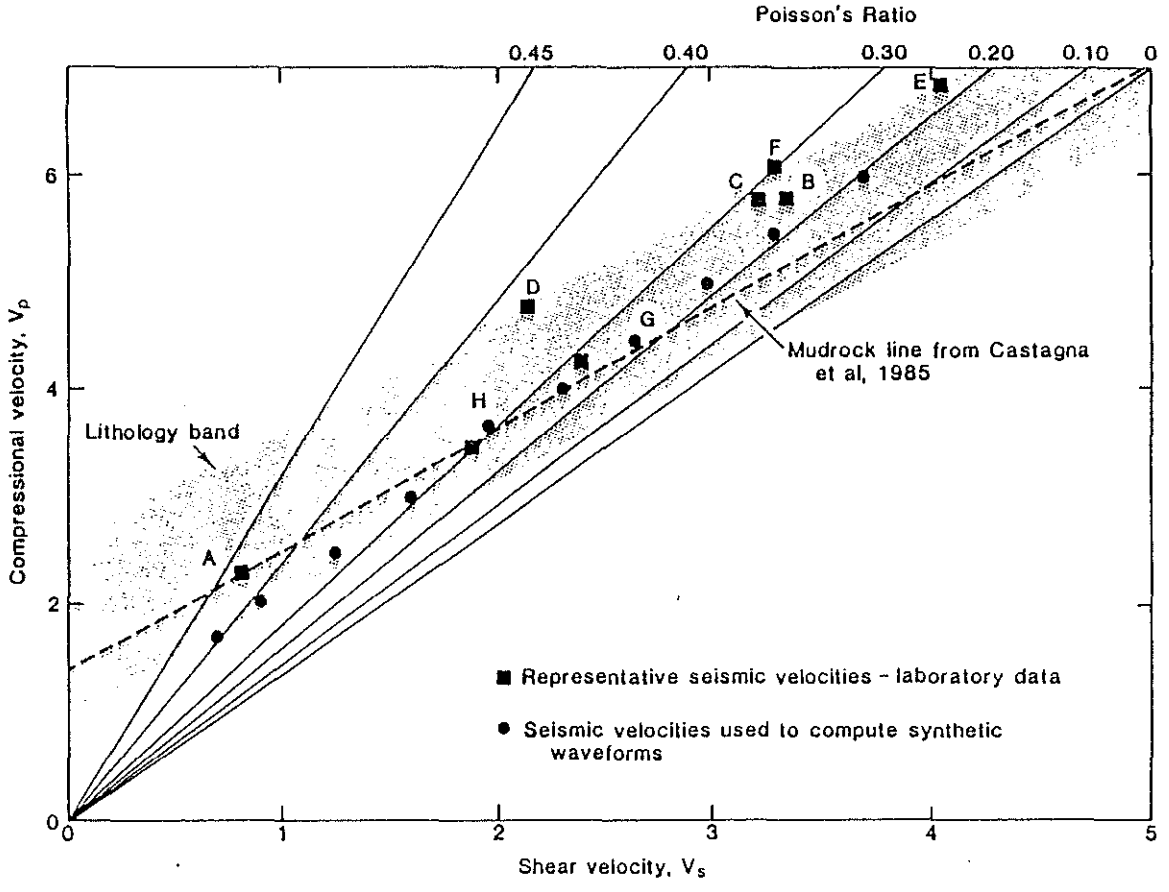

A. Shale[c]
B. Granite[c]
C. Granite[a]
D. Limestone[a]
E. Dolomite[b]
F. Basalt[c]
G. Sandstone[b]
H. Sandstone[b]

[a]Data from Nur and Simmons (1969)

[b]Data from Toksoz and others (1976)

[c]Unpublished data from Paillet

Figure 5: Trend in seismic velocities and Poisson's ratio for typical rocks, illustrating mudrock line described by Castagna et al. (1985), and lithology band described in this study.

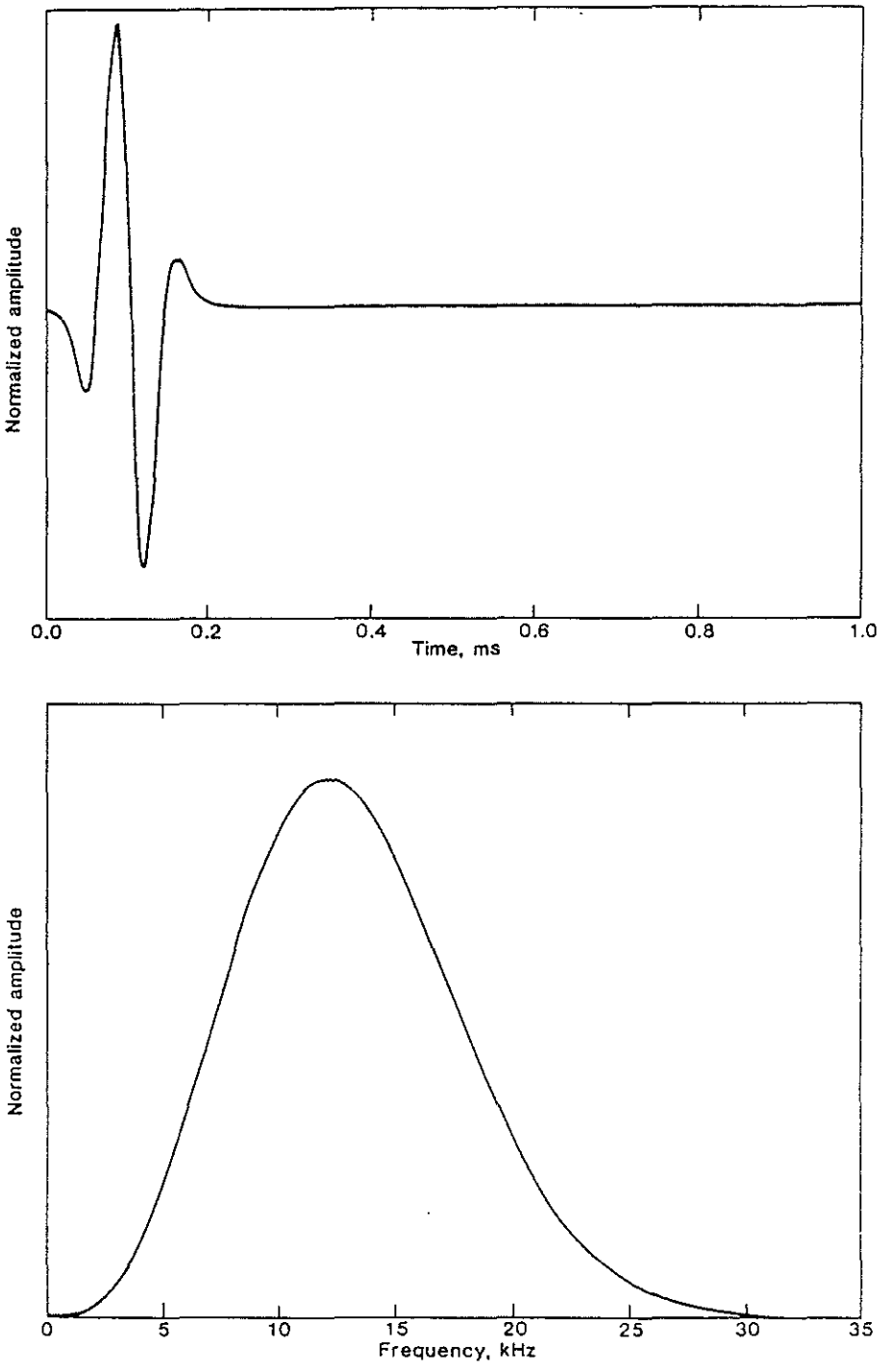

Figure 6: Acoustic energy source used in synthetic waveform computation for this study showing a) source signature; and b) source amplitude spectrum.

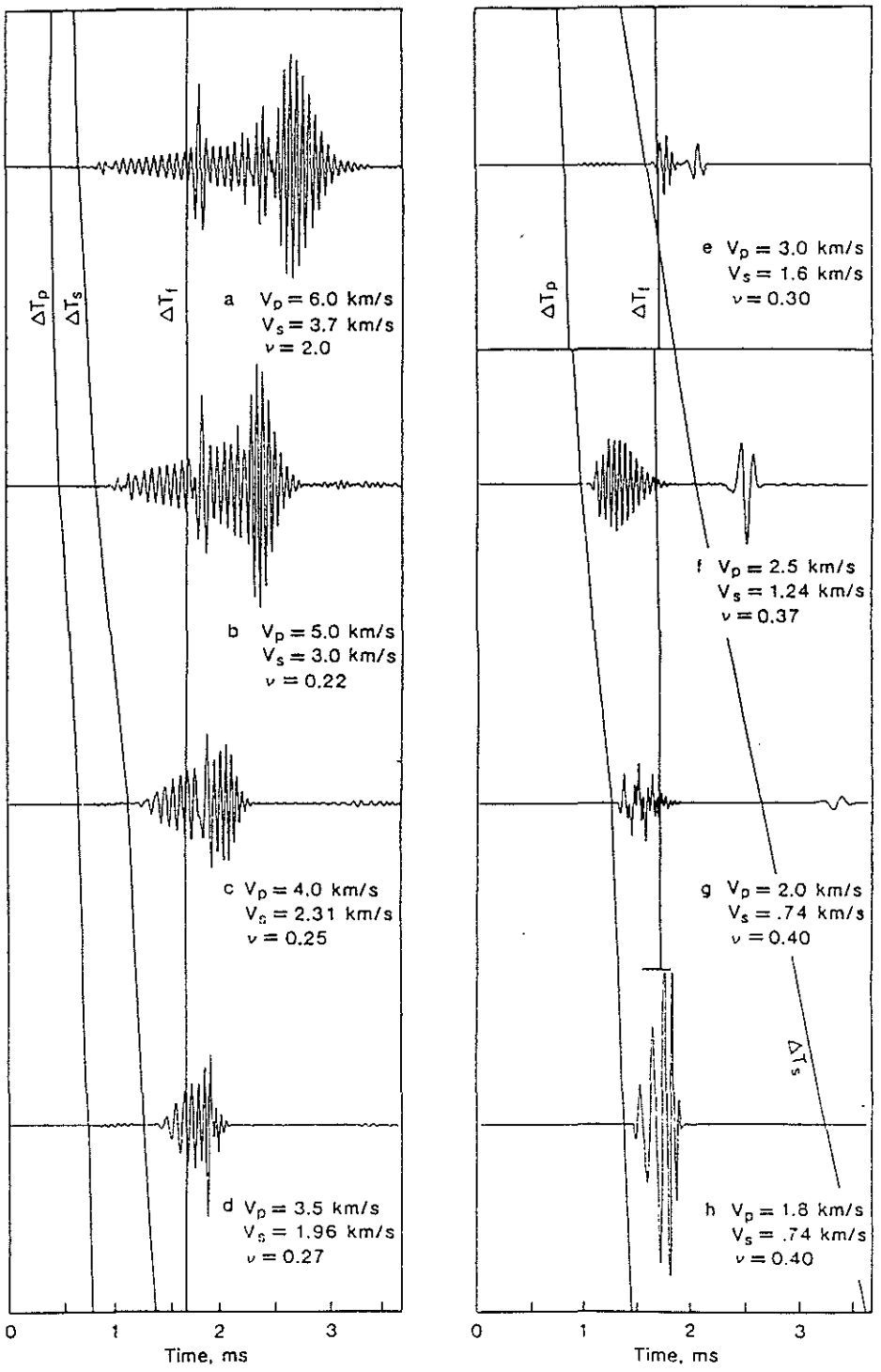

Figure 7: Synthetic waveforms computed to illustrate variation of waveform character with position along lithology band.

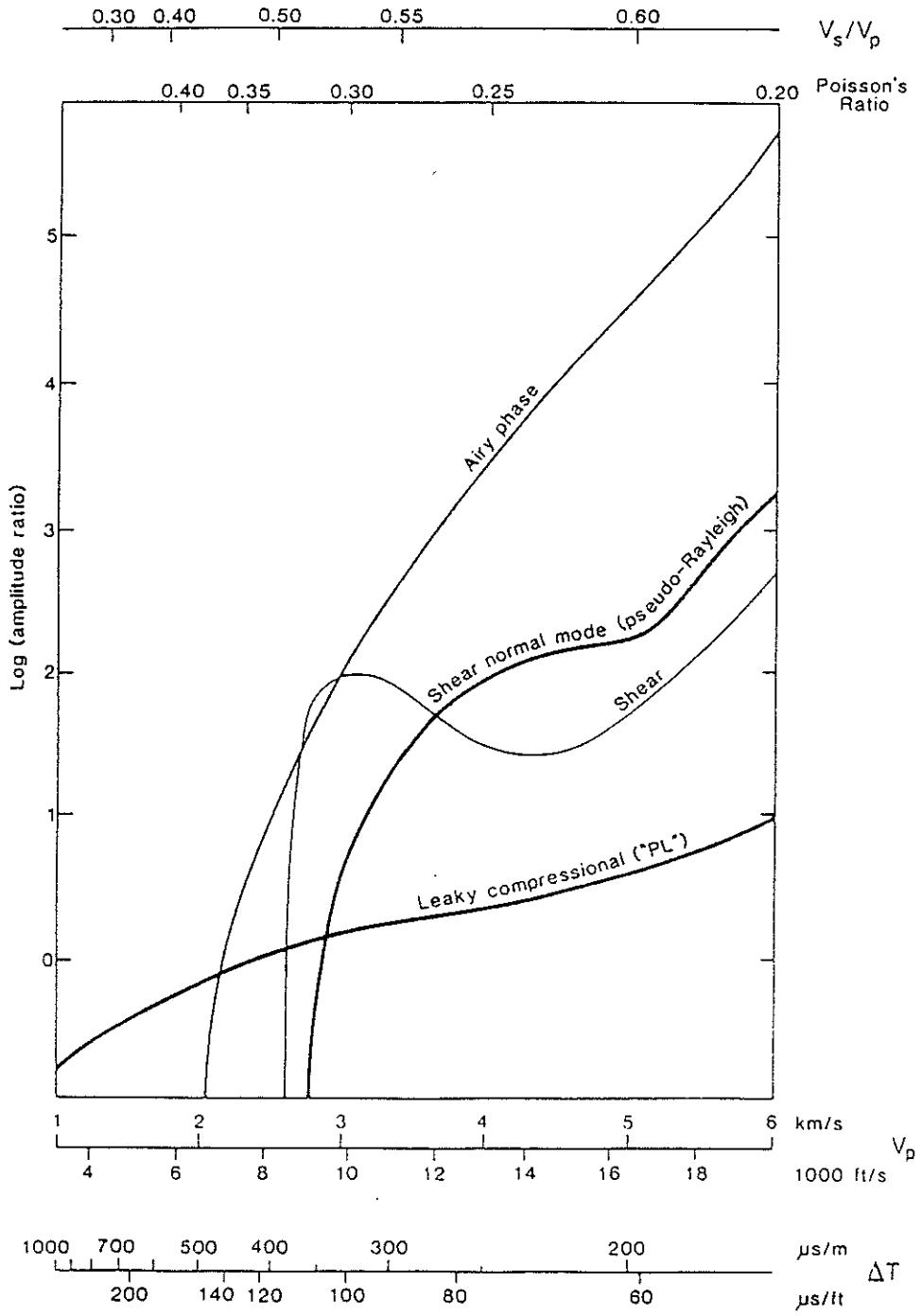

Figure 8: Mode excitation curves normalized with respect to compressional amplitude for synthetic waveforms with seismic parameters varying along the lithology band.

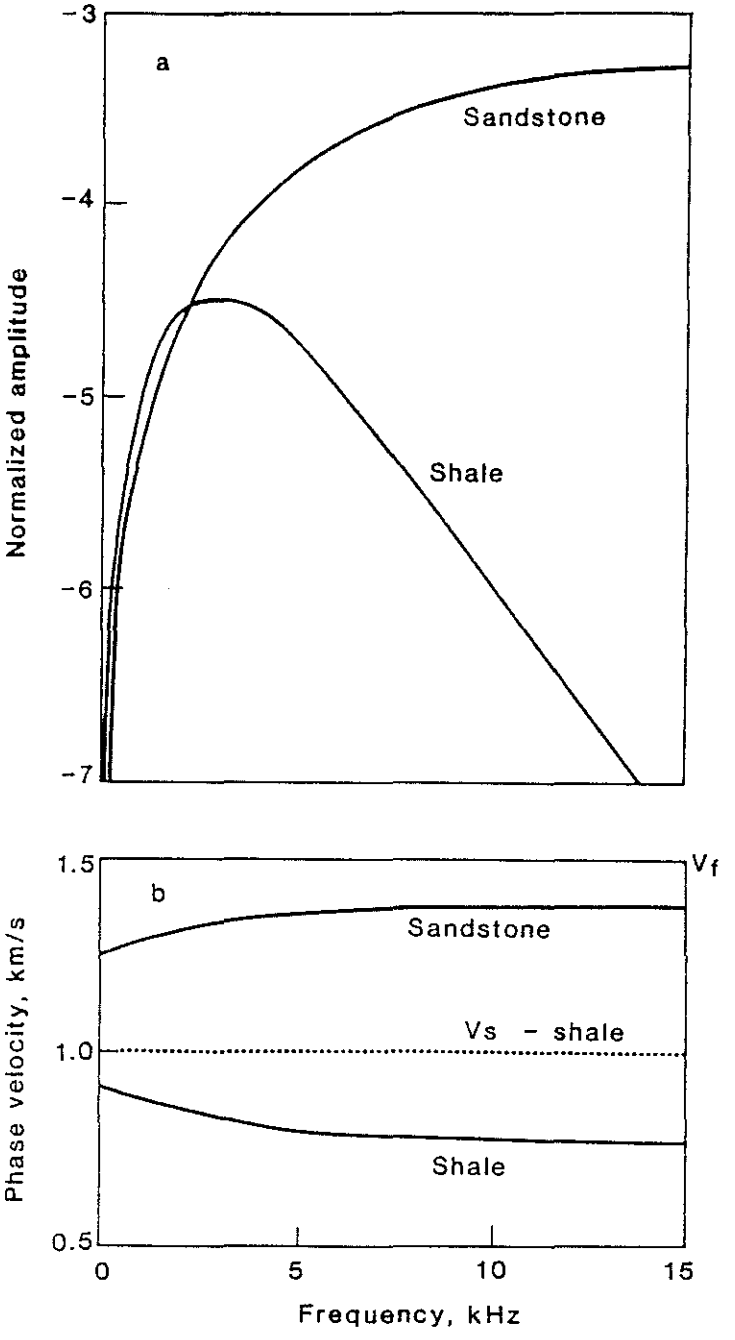

Figure 9: Comparison of predicted tube-wave excitation for a) fast rock with Poisson's ratio of 0.25; and b) slow rock with Poisson's ratio of 0.40.

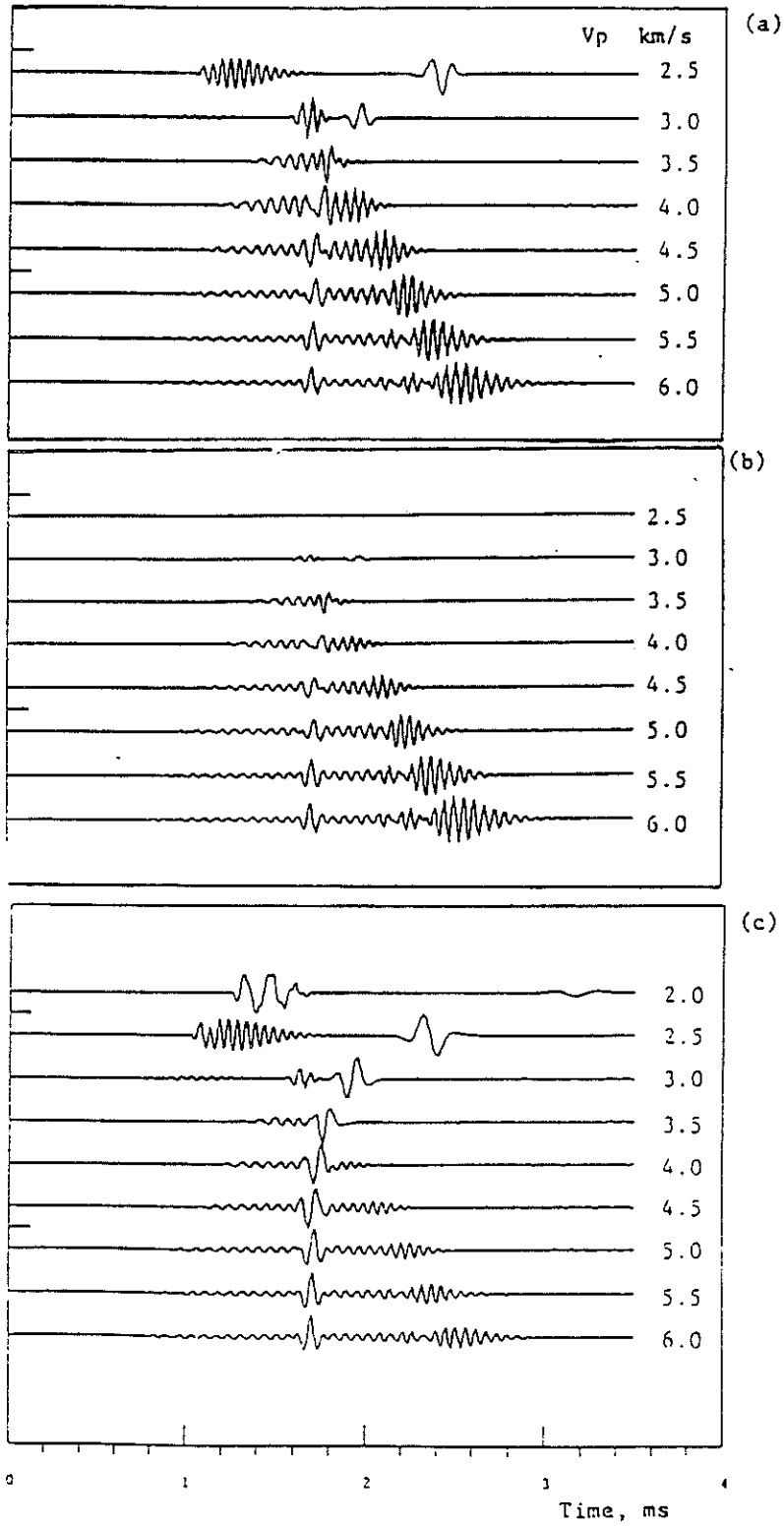

Figure 10: Synthetic waveforms computed for rock parameters varying along the lithology band and plotted on a scale typical of waveform logging equipment: a) normalized, unattenuated waveforms; b) attenuated waveforms computed using the Q values in Table 2; and c) normalized, attenuated waveforms.

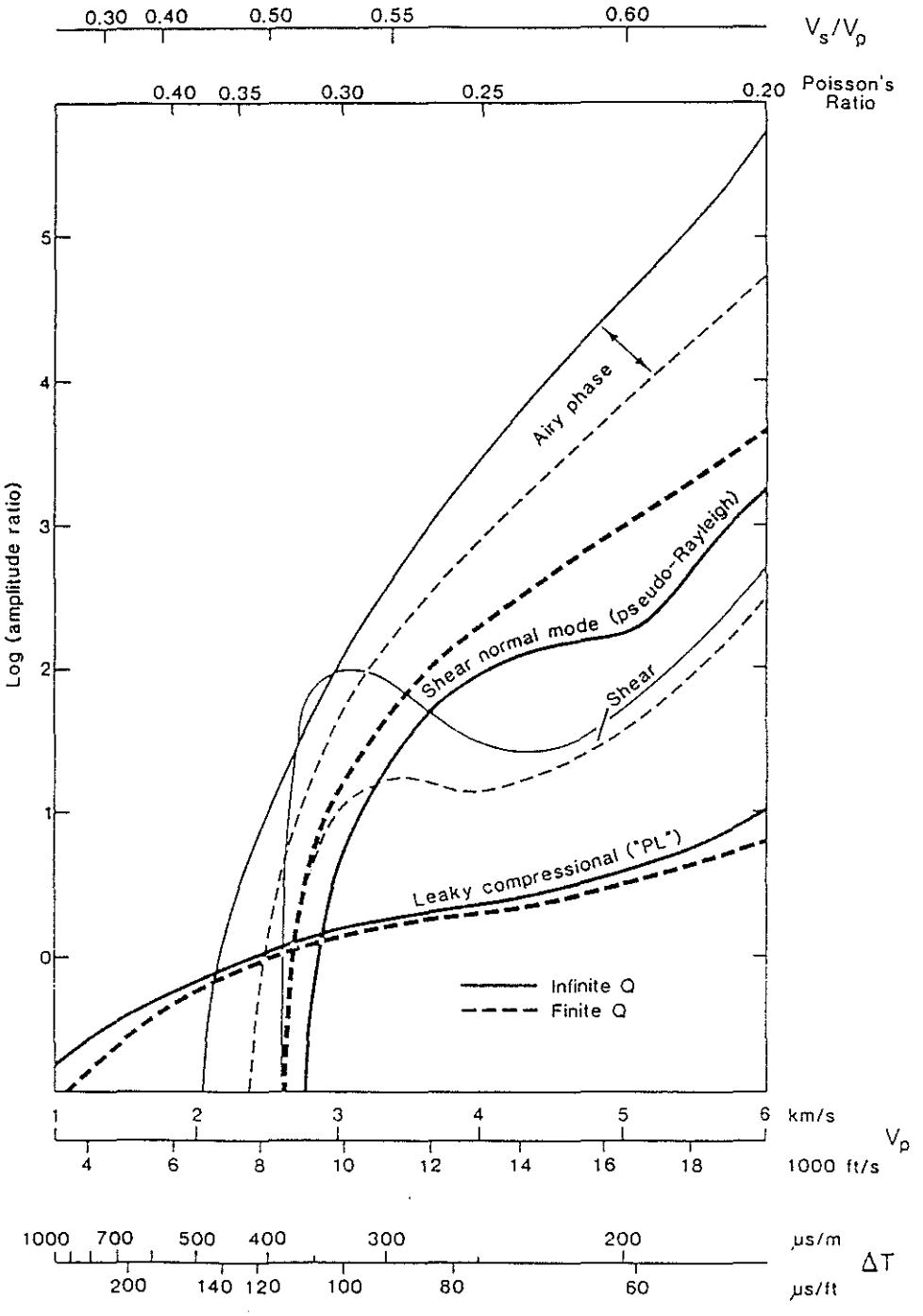

Figure 11: Effect of increasing intrinsic attenuation on mode excitation: $Q_p = 2\,Q_s$ and $Q_f = 100$.